15. Hosts were mounted in 1.34- and 1.00-mm diameter holes in white plastic squares (2 by 2 cm). Each wasp was allowed to complete examination and oviposition. The wasps were observed individually to prevent repeated parasitization of the same host. Trials in which the wasp left the host before completing oviposition were rejected.
16. Mean ± SD was used throughout. Statistical significance was determined by t tests.
17. S. E. Flanders, *Pan-Pac. Entomol.* 11, 175 (1935).
18. Head length was measured from the medial ocellus to the tip of the closed mandibles by using an ocular micrometer. Wasps differed significantly in mean head length between large and small treatment groups ($P < 0.001$).
19. Single hosts were mounted on white cardboard squares (2 by 2 cm) with gum arabic. After host examination was completed, wasps were observed as in (*15*).
20. Measurements made from films of the initial transit demonstrate a significant linear relation between wasp body length and stride length [slope, 0.58 ± 0.064 (SE); $n = 15$, $P < 0.01$].
21. Wasps were observed on single hosts mounted on cardboard cards with gum arabic. Only wasps that completed their host examination and began ovipositing were included in the data. For details of methods and results, see J. M. Schmidt and J. J. B. Smith [*J. Exp. Biol.* 129, 151 (1987)].
22. Lepidoptera: Gelechiidae.
23. We thank R. Tanner and R. Chaplinsky for technical assistance. The Natural Sciences and Engineering Research Council of Canada provided financial support.

4 March 1987; accepted 1 June 1987

The Three-Dimensional Structure of Asn^{102} Mutant of Trypsin: Role of Asp^{102} in Serine Protease Catalysis

S. SPRANG,* T. STANDING, R. J. FLETTERICK, R. M. STROUD, J. FINER-MOORE, N-H. XUONG, R. HAMLIN, W. J. RUTTER, C. S. CRAIK

The structure of the Asn^{102} mutant of trypsin was determined in order to distinguish whether the reduced activity of the mutant at neutral *p*H results from an altered active site conformation or from an inability to stabilize a positive charge on the active site histidine. The active site structure of the Asn^{102} mutant of trypsin is identical to the native enzyme with respect to the specificity pocket, the oxyanion hole, and the orientation of the nucleophilic serine. The observed decrease in rate results from the loss of nucleophilicity of the active site serine. This decreased nucleophilicity may result from stabilization of a His^{57} tautomer that is unable to accept the serine hydroxyl proton.

THROUGHOUT THE DIVERSE FAMILY of serine proteases, the three residues implicated in the bond breaking and making events of protease catalysis, His^{57}, Asp^{102}, and Ser^{195} (chymotrypsin numbering system) are conserved. The spatial relation among these residues is virtually equivalent in the three-dimensional structures of all serine proteases studied. The catalytic roles of Ser^{195} and His^{57} are firmly established (*1*). The substrate (ester or amide) carbonyl carbon undergoes a nucleophilic attack by the hydroxyl group of Ser^{195}, which leads to the formation of an acyl enzyme intermediate. His^{57} functions as a catalytic base by assisting in the transfer of a proton from the serine hydroxyl to the substrate leaving group. The role of Asp^{102} has not yet been defined. The three functions proposed for this residue are: (i) stabilizing the His^{57} conformation that is required for catalysis (*2*), (ii) stabilizing the appropriate His^{57} tautomer (*2*), and (iii) stabilizing the positively charged histidine that forms during the reaction (*3*). The proposed functions were tested with a genetically engineered mutant of the anionic isozyme of rat trypsin that was constructed by replacing Asp^{102} with an asparagine (*4*), designated here as D 102 N trypsin, where D is Asp and N is Asn.

The activity of D 102 N trypsin has been studied as a function of *p*H (*4*). The activity of this mutant enzyme toward a variety of substrates is reduced by four orders of magnitude relative to trypsin between *p*H 7 and *p*H 9, where the latter is optimally active. The Michaelis constant, K_m, of the mutant enzyme is virtually unaffected (*4*). This raises the question of whether the chemical properties of the asparagine itself or the conformational differences in the enzyme are responsible for the loss of activity in D 102 N trypsin. To address this point, we describe the three-dimensional structure of D 102 N trypsin at both *p*H 6 and *p*H 8.

Orthorhombic crystals (space group $P2_12_12_1$) of rat D 102 N trypsin grown at *p*H 6 in the presence of benzamidine were

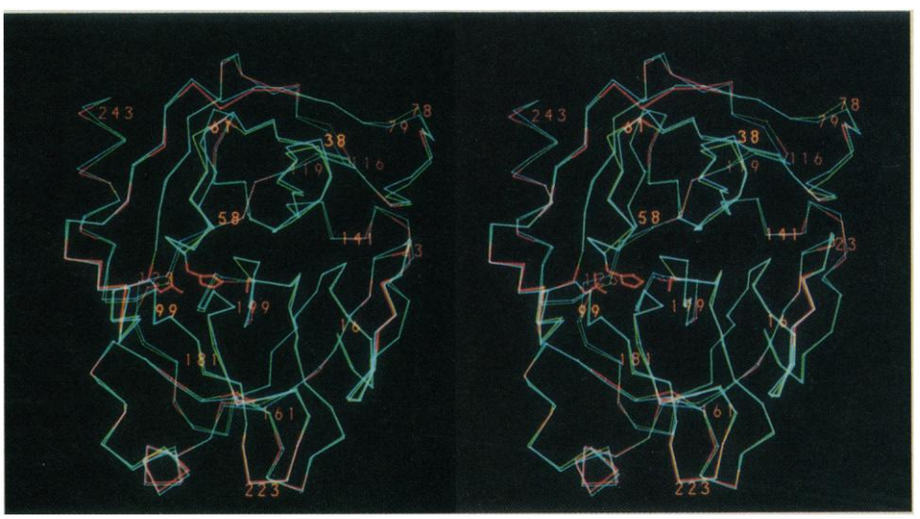

Fig. 1. An α-carbon diagram (stereoscopic) of anionic rat D 102 N trypsin at *p*H 6 (*9–12*) (green) is superimposed on bovine trypsin (blue). Residues in rat trypsin (*12*) that differ in side-chain type from corresponding residues in the bovine sequence (*25*) are highlighted in red here. Side-chain positions for residues Asn^{102}, His^{57}, and Ser^{195} are also shown in red. The root-mean-square (rms) difference in position between corresponding atoms of D 102 N rat trypsin in the crystals grown at *p*H 6 and bovine trypsin (*13, 26*) after least-squares superposition is 0.47 Å for all main-chain atoms and 0.67 Å for all side-chain atoms. Values quoted are the average of those obtained for molecules 1 and 2 in the asymmetric unit of the D 102 N trypsin crystals grown at *p*H 6. The computed rms distance may be an underestimate of the true differences in the two structures because of the use of bovine trypsin as the initial phasing model. The rms difference after superposition between all atoms of the two molecules in the asymmetric unit is 0.21 Å. The rms deviation between the main-chain atoms of the *p*H 6 and *p*H 8 crystal forms of D 102 N trypsin is 0.25 Å.

S. Sprang, T. Standing, R. J. Fletterick, R. M. Stroud, J. Finer-Moore, Department of Biochemistry and Biophysics, University of California, San Francisco, San Francisco, CA 94143.
N-H. Xuong and R. Hamlin, Department of Physics, University of California, San Diego, La Jolla, CA 92093.
W. J. Rutter, Hormone Research Institute, University of California, San Francisco, San Francisco, CA 94143.
C. S. Craik, Department of Biochemistry and Biophysics and Department of Pharmaceutical Chemistry, University of California, San Francisco, San Francisco, CA 94143.

*Present address: Howard Hughes Medical Institute, University of Texas, Dallas, TX 75235.

obtained by vapor diffusion against polyethylene glycol (Figs. 1 and 2, top). Diffraction data were measured to 2.3 Å resolution with monochromatic copper Kα radiation and the crystal cooled to 4°C on a multiwire area detector with the procedures described by Xuong *et al.* (*5*) (Table 1). A cubic crystal form (space group *I23*) was obtained at *p*H 8 by vapor diffusion against magnesium sulfate. Diffraction data for this form were recorded to 2.8 Å resolution with monochromatic copper Kα radiation on a diffractometer (*7*) (Table 1 and Fig. 2, middle). Both crystal structures were determined by molecular replacement methods (*8*) and refined by stereochemically restrained minimization of the differences between observed and computed structure amplitudes (*6, 9–12*) (Table 1 and Figs. 1 and 2).

The tertiary structures of the mutant rat anionic trypsin at both *p*H 6 and 8 are essentially identical to that of the bovine enzyme (*7, 13*). The largest differences between the enzymes from rat and cow are localized to four segments in the NH_2 terminal domain, all outside the β core, where deviations between corresponding main chain atoms exceed 1.0 Å (Fig. 1). The structural similarity between D 102 N trypsin and bovine trypsin is quite high in the neighborhood of the active site; no significant differences in the relative positions (<0.3 Å) (Table 2) or relative thermal factors are observed for Asn^{102}, Ser^{195}, or the oxyanion binding site (*14*); that is, the main-chain amide groups of residues 193 and 195. The only exception occurs in crystals grown at *p*H 6, where the side chain of His^{57} is statistically disordered (Fig. 2, top) (*11, 12*), and is partitioned between the gauche conformation observed in native trypsin and an alternative trans conformation, in which the imidazole side chain is displaced from the active site toward the solvent. Only the native gauche His^{57} conformation is observed in crystals grown at *p*H 8. Unless otherwise stated, all references to His^{57} in the following discussion refer to the native conformer.

In both the *p*H 8 and *p*H 6 crystal forms, Asn^{102} is superimposable within experimental error with Asp^{102} of the bovine enzyme (Fig. 2). In trypsin, one of the carboxylate oxygen atoms of Asp^{102} accepts hydrogen bonds from the main-chain amide groups of residues 56 and 57, and the second accepts hydrogen bonds from both the Nδ1 atom of

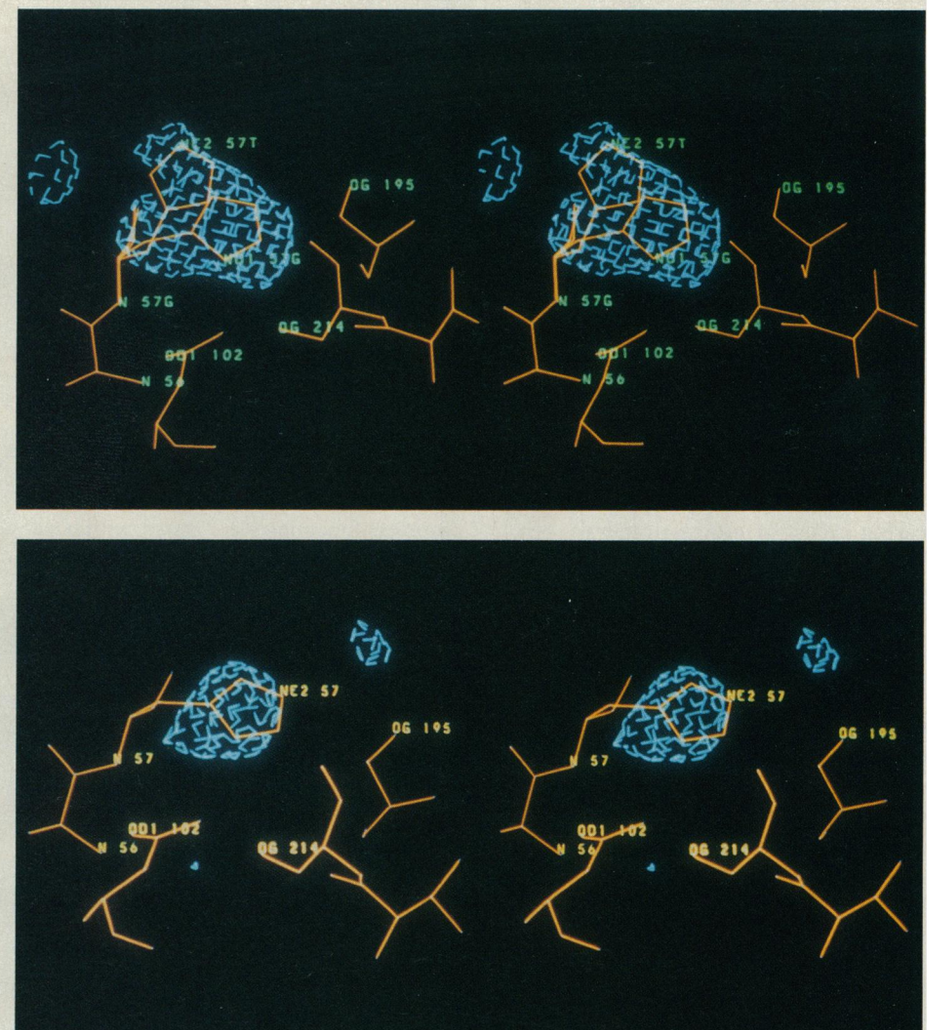

Fig. 2. (**Top**) The difference Fourier map ($F_{obs} - F_{calc}$) at the catalytic site of D 102 N rat trypsin at *p*H 6. The side-chain atoms of His^{57} were omitted from the calculated structure factors and phases. The trans and gauche conformations of the histidine side chain related by χ^1 torsional differences of 70° are superimposed on the electron density. The difference electron density is shown at a contour level of 0.2 electron per cubic angstrom. The map extends over all atoms shown in the figure. No negative density is present in this region at the 0.2 electron per cubic angstrom level. Two lobes of flat, ellipsoidal density are evident, both continuous with the density corresponding to the Cβ atom of His^{57}. The peaks are of unequal magnitude; the stronger peak is located within the active site between the side chains of Asn^{102} and Ser^{195} at a position coincident with His^{57} in the structures of bovine trypsin, and the second weaker peak is outside of the active site pocket. The shape of both lobes of density and their proximity to the Cβ atom of His^{57} rules out the assignment of either peak to ordered solvent. (**Middle**) A difference Fourier map ($F_{obs} - F_{calc}$) showing the catalytic site of D 102 N trypsin from crystals grown at *p*H 8. The side-chain atoms of His^{57} were omitted from the calculated structure factors and phases. At this *p*H, only the gauche conformer for His^{57} is observed in the difference electron density. The histidine conformation is almost identical to that observed in bovine trypsin–benzamidine complex (*7*). The structure of D 102 N trypsin at *p*H 8 was determined by molecular replacement, using the refined structure at *p*H 6 as a search model. The side-chain atoms of Asn^{102}, His^{57}, and Ser^{195} as well as solvent, benzamidine, and calcium ion atoms were omitted from this model. The rotation function produced only one significant peak and was evaluated with all data to 2.8 Å and an integration radius from 4.0 to 16 Å. The *R* factor at the correct translation position was 0.35. A difference Fourier map computed with phases from the molecular replacement solution revealed the positions of the omitted side chains, calcium ion, and benzamidine molecule. These were included in the phasing model and the structure was subjected to 23 cycles of stereochemically restrained crystallographic refinement (Table 1) (*6*). (**Bottom**) The bovine trypsin structure (thin lines) is superimposed on that of D 102 N rat trypsin crystallized at *p*H 6.0 (thick lines). Both conformers of His^{57} in D 102 N rat trypsin are shown.

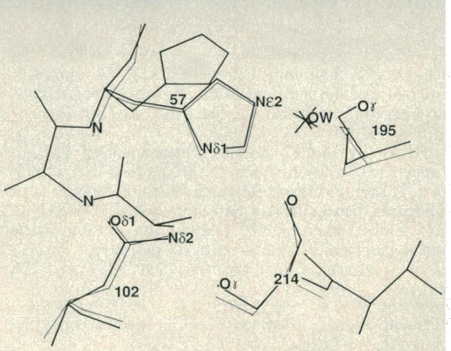

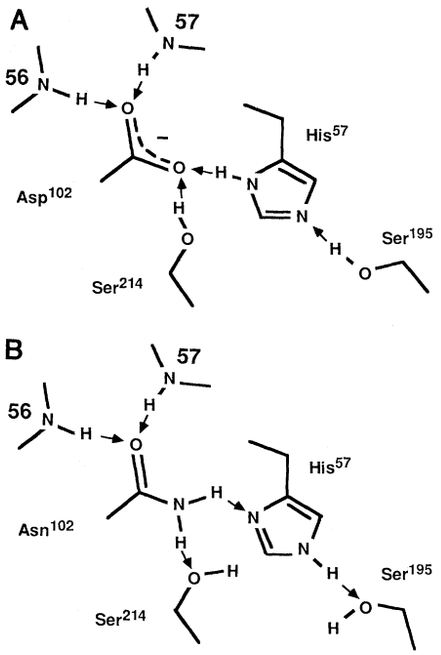

Fig. 3. (**A**) In the hydrogen bond network found in D 102 N trypsin above neutral *p*H, His^{57} is unable to accept a proton from Ser^{195} Oδ. The orientation of the hydrogen bond between His^{57} and Ser^{195} is the reverse of that observed in the bovine trypsin–benzamidine structure (*7*). (**B**) In the hydrogen bond network of wild-type trypsin, His^{57} is an acceptor for the proton from Ser^{195}.

Table 1. Crystal and diffraction data for D 102 N trypsin. The diffraction data for the crystals grown at *p*H 6 were collected with an area detector, whereas the data for the crystals grown at *p*H 8 were collected with a diffractometer.

Diffraction data	Crystal form	
	*p*H 6	*p*H 8
Crystal data		
Space group	$P2_12_12_1$	*I*23
Cell dimensions (Å)	*a* = 40.4 *b* = 92.0 *c* = 127.4	*a* = 124.4
Molecules per asymmetric unit	2	1
Diffraction data		
Resolution (Å)	2.3	2.8
Total observations	90,000	5,000
Unique observations	22,000	4,500
R_{symm}*	0.05	
Refinement results		
R_{cryst}†	0.16	0.21
Resolution (Å)	6.0–2.3	8.0–2.8
rms difference (bond) (Å)‡	0.03	0.03
rms difference (angle) (Å)‡	0.05	0.05

*Agreement between symmetry-related structure-factor magnitudes *R*

$$R = (\Sigma_h \Sigma_i |\langle F_h \rangle - F_{hi}|)/(\Sigma_h F_h)$$

where $\langle F_h \rangle$ is the mean structure factor magnitude of the *i* observations of reflections that are related to the Bragg index *h*. †Agreement between the observed (F_{obs}) and calculated (F_{calc}) structure factor magnitudes R_{cryst}

$$R_{cryst} = (\Sigma||F_{obs}| - |F_{calc}||)/(\Sigma |F_{obs}|)$$

‡Root-mean-square deviation between the ideal and refined bond distances and angle distances.

His^{57} and the Oγ atom of Ser^{214} (Table 2 and Fig. 3). In D 102 N trypsin, there are two chemically distinct conformations possible for Asn^{102}. In one of these the Nδ2 group of Asn^{102} would be oriented toward the main-chain amide groups of residues 56 and 57. Since the asparagine amido group cannot form a hydrogen bond with the main-chain amides in this orientation, they could approach no closer than the sum of their van der Waals radii (>3.4 Å).

The alternative conformation is related to the first by a rotation of 180° about the Cβ–Cγ bond. In this case, the Oδ1 atom of asparagine could accept hydrogen bonds from the main-chain amide groups, whereas the Nδ2 atom could accept hydrogen bonds from the His^{57} imidazole and Ser^{214} hydroxyl groups. The two conformations can be distinguished by the observed distances between the main-chain amides of residues 56 and 57 and the nearest atom of the Asn^{102} side chain. The interatomic distances in the present model (*15, 16*) support the assignment of the tautomeric form shown in Fig. 3A. One of the Asn^{102} amido atoms is located 2.6 Å from the amide nitrogen of residue 56 and 3.1 Å from the amide of residue 57. This atom of the Asn^{102} side chain could then be involved in hydrogen bonds with these two amides and would thus be identified as Oδ1. Asn^{102} Nδ2 would therefore be a hydrogen bond donor to both the Nδ1 of His^{57} and the Oδ of Ser^{214}. Asp^{102} accepts hydrogen bonds from both of these residues in bovine trypsin.

In the proposed crystallographic model, Asn^{102} can only serve as a hydrogen bond donor to His^{57}; the polarity of the hydrogen bond network involving His^{57}, residue 102, and Ser^{195} is reversed in the mutant enzyme with respect to that in bovine trypsin (Fig. 3). For values of *p*H greater than the pK_a of the imidazole (K_a is the ionization constant), the monoprotonated tautomer must be protonated at Nε2 since it serves as a hydrogen bond acceptor from Asn^{102} at Nδ1. In contrast to trypsin, the Nε2 of His^{57} in the mutant enzyme is a potential hydrogen bond donor to the Oγ of Ser^{195}. Thus His^{57} cannot act as a general base in transferring a proton from Ser^{195} and this probably accounts for the diminished activity of D 102 N trypsin near neutral *p*H. For trypsin above neutral *p*H, where the enzyme becomes active, His^{57} is protonated at Nδ1 (*17*). Therefore, the presence of a negatively charged Asp^{102} maintains the unprotonated Nε2 with a lone pair of electrons as the general base catalyst for transfer of the proton from the Oγ of Ser^{195} to the leaving group.

A difference Fourier map (Fig. 2, top) for the crystals grown at *p*H 6 was computed with the histidine omitted from the calculated phases and structure factors, revealing two sites for the side chain (*11, 12*). In one of these, the Cβ–Cγ bond is trans to Cα–N, and the imidazole is rotated from the catalytic site. The trans His^{57} conformer does not form a hydrogen bond with Asn^{102} or Ser^{195} but rather is in contact with a solvent water molecule at the surface of the enzyme (Table 2). The alternative position is nearly gauche and similar to the His^{57} conformation in bovine trypsin and D 102 N trypsin crystallized at *p*H 8 (Fig. 2, bottom).

Integration of the difference electron density indicates that the occupancy ratio of the gauche to trans isomers is approximately 2 to 1 (Fig. 2, top) (*11, 12*). A difference map computed with phases derived from all of the atoms in the refined model reveals residual positive electron density in the vicinity of the Cε1 of His^{57} (gauche), and may correspond to a partially occupied solvent water which is present in the active site pocket when His^{57} is displaced (trans).

The displacement of His^{57} from the active site of D 102 N trypsin below neutral *p*H is probably a consequence of steric conflicts between the protonated Nδ1 atom of His and the proton on the Nδ2 of Asn. D 102 N trypsin, like its natural homolog, is crystallized only in the presence of the substrate analog benzamidine, and there are no appar-

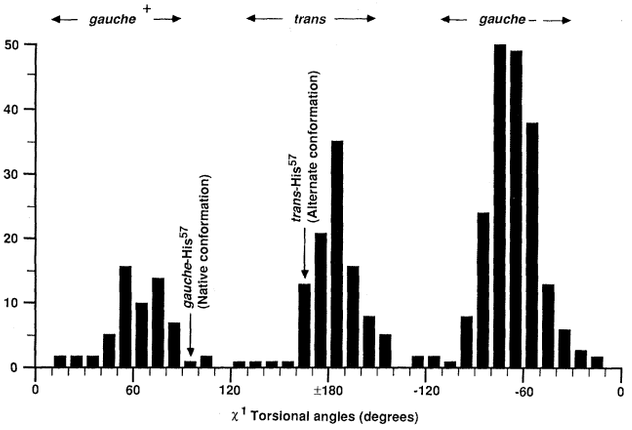

Fig. 4. A histogram showing the χ^1 torsion angles of 353 histidines found in 53 protein structures refined to greater than 2.0 Å resolution (*11, 26*). The χ^1 angle of 92° gauche observed in His^{57} of bovine trypsin is rare. Angle values are trimodally distributed about +60°, 180°, and −60°. The trans conformer that occurs at *p*H 6 in D 102 N rat trypsin is more frequently observed.

Table 2. Conformational and stereochemical data for active site residues in bovine and D 102 N trypsins. Values for the two molecules in the asymmetric unit of D 102 N trypsin grown at *p*H 6 are averaged. Distances are not given for the 2.8 Å resolution crystals grown at *p*H 8. The wild-type coordinates are from the bovine trypsin–benzamidine crystal structure (*7*).

Residue	Atoms	Conformational angles (degrees)		Hydrogen bond distance (Å)	
		Asn^{102}	Wild type	Asn^{102}	Wild type
His^{57} (gauche)	N–Cα–Cβ–Cγ	84	92		
(trans)		157			
His^{57} (gauche)	Cα–Cβ–Cγ–Nδ1	−96	−100		
(trans)		−93			
Ser^{195}	N–Cα–Cβ–Oγ	−59	−77		
His^{57} (gauche)	Nδ1–Asn/Asp^{102} N/Oδ2			2.8	2.7
His^{57} (gauche)	Nε2–Ser^{195} Oγ2			3.2	3.0
His^{57} (gauche)	Nε2–H_2O^{293}O			3.0	
Asn^{102}/Asp^{102}	Oδ1–Ala^{56}N			2.6	2.9
Asn^{102}/Asp^{102}	Oδ1–His^{57}N			3.1	2.8
Asn^{102}/Asp^{102}	N/Oδ2–Ser^{214}Oγ			2.7	2.8
Ser^{195}	Oγ–H_2O^{710} O			2.9	3.0

ent steric conflicts between His^{57} and other residues in the catalytic site. However, even in trypsin, the native gauche conformation of His^{57} imidazole may be energetically unfavored and require hydrogen bond stabilization by Asp^{102}. A survey of the χ^1 angles of His side chains in refined protein structures (Fig. 4) shows that the conformation found in bovine trypsin is uncommon. Steric hindrance arises as a result of close contacts between the Cγ and Cδ2 imidazole atoms and the main-chain carbonyl carbon [contact distances of 3.0 Å and 3.2 Å, respectively, are measured from the coordinates of bovine trypsin (*7*)]. Nevertheless, His^{57} is well ordered in crystals of native trypsin (*13, 17*) and tritium exchange measurements indicate that expulsion of His^{57} from the active site pocket occurs in solution with a frequency of less than 1 in 50 over the *p*H range 1.5 to 9 (*18*). Displacement of His^{57} from the gauche conformation in serine protease crystals has so far been seen to occur as a result of steric conflict in covalent intermediates formed with certain substrate analogs (*19, 20*) or as a result of the introduction of heavy metals into the active site (*21, 22*). In native trypsin, the histidine conformation is stabilized by a hydrogen bond between the Nδ1 atom of His and the carboxylate oxygen atom of Asp^{102}.

In D 102 N trypsin, the conformation of His^{57} appears to be linked to its protonation state. In the monoprotonated imidazole tautomer that predominates above neutral *p*H, the Nδ1 atom of His can accept a hydrogen bond from Nδ2 of Asn^{102}. Protonation at the histidine Nδ1 at the lower *p*H results in the loss of this hydrogen bond and possibly also steric conflict with the Nδ2 of Asn^{102}. The imidazole is then free to rotate to the more favored trans conformation, away from the catalytic site. Orthorhombic crystals of D 102 N trypsin are grown near the pK_a of histidine, and thus the statistically disordered histidine side chain may reflect an equilibrium distribution of mono (gauche) and diprotonated (trans) forms of the His^{57} imidazole. The variant D 102 N trypsin is able to react with the active site titrant tosyl-L-lysine chloromethyl ketone (TLCK) at 20 to 70% of the rate observed for trypsin from *p*H 7.2 to 8.7 (*4*), which suggests that as in the *p*H 8 crystals, a substantial proportion of D 102 N trypsin molecules in solution contain His^{57} in the native gauche conformation.

As a result of the substitution of Asn for Asp^{102}, the mutant trypsin reacts with diisopropylfluorophosphate (DFP), a reagent that specifically titrates the Ser^{195} nucleophile, 10^4 times more slowly than with trypsin (*4*). The decreased Ser^{195} nucleophilicity in D 102 N trypsin probably results from the lack of a base in the active site to accept the serine hydroxyl proton. His^{57} does not act as a base in this mutant because it exists in the incorrect tautomer. While the tautomeric form of His^{57} is changed in D 102 N trypsin, the oxyanion binding site (*14*)—the main-chain amide groups of residues 193 and 195—is unaltered. The reduced activity of the mutant thus gives an upper limit to the contribution of transition state binding alone to the reaction rate. Trypsin normally accelerates the rate of DFP hydrolysis by a factor of 10^8 (*20*). Our results suggest that a factor of 10^4 in rate enhancement may derive from the stabilization and orientation of the lone pair on the Nε2 atom of His^{57}. The remaining factor of 10^4 can presumably be ascribed to orientation of the nucleophile (Ser^{195}) and transition state binding. Under alkaline conditions (*p*H > 10), the rate of catalysis by the mutant approaches 10% of that of the native enzyme (*4*) through an altered mechanism in which base catalysis appears to be provided by solvent hydroxide. In trypsinogen, the situation is reversed; His^{57} is correctly oriented, but the oxyanion binding site is not properly formed to stabilize the transition state (*21*), even after irreversible binding of the transition state analog DFP (*23*). The reaction rate toward DFP is also reduced by a factor of ~10^4 relative to trypsin (*20*), which again ascribes an upper limit of 10^4 rate acceleration to transition state binding. Catalytic rate enhancement by serine proteases is thus partitioned almost equally between (i) orientation and stabilization of the enzyme base His^{57} and (ii) the correctly oriented serine nucleophile and transition state binding site. Studies of D 102 N trypsin indicate that the Asp^{102} residue plays a critical role in the first of these processes, perhaps electronically with His^{57} (*24*), and structurally, by providing hydrogen bond stabilization of the functional tautomer and thus maintaining its correct orientation within the catalytic site.

REFERENCES AND NOTES

1. G. Dixon, S. Go, H. Neurath, *Biochim. Biophys. Acta* **19**, 193 (1956); E. Shaw, M. Mares-Guia, W. Cohen, *Biochemistry* **4**, 2219 (1965).
2. W. W. Bachovchin, *Biochemistry* **25**, 7751 (1986).
3. A. R. Fersht and J. Sperling, *J. Mol. Biol.* **74**, 137 (1973); A. R. Fersht, *Enzyme Structure and Mechanism* (Freeman, New York, ed. 1, 1977).
4. C. S. Craik *et al.*, *Science* **237**, 909 (1987).
5. N. H. Xuong, S. T. Freer, R. Hamlin, C. Nielsen, W. Vernon, *Acta Crystallogr.* **A34**, 289 (1978); R. Hamlin *et al.*, *J. Appl. Crystallogr.* **14**, 85 (1981); A. J. Howard, C. Nielsen, N. H. Xuong, *Methods Enzymol.* **114**, 452 (1985).
6. W. A. Hendrickson and J. H. Konnert, in *Computing in Crystallograpky*, R. Diamond, S. Rameseshan, K. Venkatesan, Eds. (Indian Academy of Sciences, Bangalore, 1980), p. 13.01. The program PROLSQ written by Hendrickson and Konnert was used for refinement. The modification added to PROLSQ by B. Finzel was used to decrease computation time.
7. J. L. Chambers and R. M. Stroud, *Acta Crystallogr.* **B33**, 1824 (1977); *ibid.* **B35**, 1861 (1979); M. Krieger, L. M. Kay, R. M. Stroud, *J. Mol. Biol.* **83**, 209 (1974).
8. M. G. Rossmann, Ed., *The Molecular Replacement Method* (Gordon & Breach, New York, 1972); R. A. Crowther, *ibid.*, p. 173.
9. The structure of D 102 N rat trypsin at *p*H 6 was determined by molecular replacement methods (*8*) by using the atomic coordinates of bovine trypsin-benzamidine (*7*) as a search set. The coordinates were modified by removal of all side-chain atoms for positions at which rat and bovine trypsins differ in amino acid sequence, as well as those of His^{57} and Ser^{195}. Coordinates for solvent (benzamidine) and the bound calcium ion were excluded. The crystals grown at *p*H 6 exhibit pseudotranslational symmetry such that the unit cell comprises a *b* axis repeat of two $P2_12_12_1$ subcells related by a translation of *b*/2. As a consequence, reflections with *h* odd for $\infty \geq d \geq 3.0$ Å are systematically weak or absent. The relative rotation of the search coordinates with respect to the rat trypsin unit cell was determined by using the fast rotation function developed by Crowther (*8*). The correct solution was found with data to 3.0 Å resolution and an integration radius from 4.5 Å to 16.0 Å. The position of the rotated search model in the D 102 N trypsin unit cell was found by an *R*-factor search (with a program obtained from E. Dodson and P. Evans), which gave an *R* factor of 0.43. The position was refined by least

squares with the computer program CORELS (*10*). The positional parameters of individual atoms were then refined subject to stereochemical restraints by using the subcell data (*6*). The positions of missing side-chain atoms and those of the benzamidine and calcium were determined from the subcell difference electron density map computed from the refined model. A model of the full crystallographic asymmetric unit in the correct $P2_12_12_1$ unit cell was then constructed by adding a replicate of the trypsin molecule translated by 46 Å along the *b* and 32 Å along *c*. The full model was refined in three stages. In each stage the model was refit to a difference Fourier map computed with the coefficients $(2F_{obs} - F_{calc})$. Strong peaks in the electron density in positions consistent with hydrogen bond contacts to the protein or other established solvent positions were included in the model as ordered solvent. Next, the positional and thermal parameters of all atoms were refined by iterations of restrained crystallographic least squares, with data in the resolution range 6 Å $\leq d \leq$ 2.3 Å. Refinement was stopped when further cycles failed to reduce the crystallographic *R* factor and when the mean shift in coordinate positions was less than 0.05 Å. Refined coordinates were then used to compute phases for a new electron map to be used in the next stage of manual refitting. After the third stage (*R* factor = 0.18), examination of the electron density failed to reveal errors or ambiguity in main- or side-chain positions, although the side chains of six residues located at the surface of the molecules were disordered and could not be defined. Up to this point, side-chain atoms for His^{57}, Asn^{102}, or Ser^{195} had been excluded from the model. A difference electron density map $(F_{obs} - F_{calc})$ revealed strong and well-ordered density for the Asn^{102} and Ser^{195}, but the His^{57} residue appeared to be statistically disordered (Fig. 2, top) (*11*).

10. J. L. Sussman, S. R. Holbrook, G. M. Church, S. H. Kim, *Acta Crystallogr.* **A32**, 311 (1976).
11. The possibility that one or other of the peaks are artifactual was tested by independent refinement of two alternative models: one with His^{57} fit to the stronger, internal density and the second with His^{57} fit to the external density. In each model the His^{57} atoms were assigned full occupancy and side-chain positions for Asn^{102} and Ser^{195} were included. Each model was subjected to restrained crystallographic refinement by varying the thermal and positional parameters of all atoms. Subsequently, a difference Fourier map $(F_{obs} - F_{calc})$ was computed for each model with the use of the refined positional and thermal parameters for all of the atoms in the respective models. In both cases, residual electron density appeared at the alternative histidine site. Again, the observed density peaks were contiguous with the Cβ atom of His^{57} and thus could not be interpreted as ordered water molecules. The relative occupancy of the two histidine positions and the total occupancy of both positions relative to other histidine side chains was estimated by integration of difference electron density at all of the histidine side-chain positions in one of the trypsin molecules in the asymmetric unit. The difference Fourier map $(F_{obs} - F_{calc})$ used in the integration was computed from a model in which the side-chain atoms of all four histidine residues (at sequence positions 40, 57, 70, and 87) were removed from the coordinate set of one molecule. Integration was performed manually by summing over all grid points within 2.0 Å of histidine atomic positions that had electron density at least one standard deviation greater than the background density. After normalization the apparent relative integrated difference densities at the histidine side-chain positions were: His^{40}, 0.87; His^{57}, 0.60; His^{70}, 0.79; and His^{87}, 1.0. All but His^{57} are well ordered, so the range in integrated densities reflects thermal motion and experimental error. The sum of the density over the two His^{57} side-chain sites is lower than the mean density of the well-ordered histidine side chains, but is consistent with the high B factors of His^{57} atoms at both positions. The relative occupancy of the alternative His^{57} positions was estimated by integrating the difference density at the Nδ1 and Cε1 atoms of the gauche conformer and the Cδ2 and Nε2 atoms of the trans conformer and by taking the ratio of the integrated densities for the two positions. The remaining histidine atoms were not included in the integration because the resolution of the data set did not allow the densities of the two conformers to be resolved at those positions.

Final refined positional and thermal parameters for both trans and gauche conformers were determined by refining an atomic model in which both conformers were simultaneously included. Side-chain atoms of the gauche conformer were assigned occupancies of 0.67 and atoms of the trans isomer were assigned occupancies of 0.33 based on the estimate derived from the integration described above (*12*). After three final cycles of refinement of all thermal and positional parameters of both trypsin monomers in the asymmetric unit, the crystallographic *R* factor was 0.161.

12. A modified version of PROTIN (obtained from J. Smith) does not generate restraints between alternate side-chain positions of a statistically disordered residue. This allows refinement of two conformations of an amino acid simultaneously.
13. W. Bode and P. Schwager, *J. Mol. Biol.* **98**, 693 (1975).
14. R. Henderson, *ibid.* **54**, 341 (1970).
15. An upper estimate of the mean error in atomic position is 0.25 Å. It was obtained by an analysis of the variation of crystallographic *R* factor as a function of resolution (*16*).
16. V. Luzatti, *Acta Crystallogr.* **6**, 142 (1953).
17. A. A. Kossiokoff and S. A. Spencer, *Biochemistry* **20**, 6462 (1981).
18. M. Krieger *et al.*, *ibid.* **15**, 3458 (1976).
19. M. N. G. James, A. R. Sielecki, G. D. Brayer, L. T. Delbaere, C. A. Bauer, *J. Mol. Biol.* **144**, 43 (1980).
20. P. H. Morgan *et al.*, *Proc. Natl. Acad. Sci. U.S.A.* **69**, 3312 (1972).
21. A. A. Kossiakoff *et al.*, *Biochemistry* **16**, 654 (1977); H. Fehlhammer, W. Bode, R. Huber, *J. Mol. Biol.* **111**, 415 (1977).
22. J. L. Chambers *et al.*, *Biochem. Biophys. Res. Commun.* **59**, 70 (1974).
23. M. O. Jones and R. M. Stroud, *Biochemistry*, in press.
24. D. M. Blow *et al.*, *Nature (London)* **221**, 337 (1969).
25. C. S. Craik *et al.*, *J. Biol. Chem.* **259**, 14255 (1984).
26. The coordinates were obtained from the Protein Data Bank at Brookhaven National Laboratory.
27. We thank J. Sadowsky, C. Neilsen, and E. Goldsmith for assistance with Area Detector data collection and processing and B. Montfort for assistance with crystallographic refinement calculations. We gratefully acknowledge grant support from NIH: AM31507 to S.R.S., GM24485 to R.M.S., and AM26081 to R.J.F.; from NSF: DMB8608086 to C.S.C. and PCM830610 to W.J.R.; a Bristol Meyer grant of Research Corporation and a CCRC grant to C.S.C. The coordinates of the D 102 N trypsin structure at *p*H 6 have been submitted to the Protein Data Bank at Brookhaven National Laboratory.

29 September 1986; accepted 29 May 1987

The Catalytic Role of the Active Site Aspartic Acid in Serine Proteases

CHARLES S. CRAIK, STEVEN ROCZNIAK,* COREY LARGMAN,† WILLIAM J. RUTTER

The role of the aspartic acid residue in the serine protease catalytic triad Asp, His, and Ser has been tested by replacing Asp^{102} of trypsin with Asn by site-directed mutagenesis. The naturally occurring and mutant enzymes were produced in a heterologous expression system, purified to homogeneity, and characterized. At neutral *p*H the mutant enzyme activity with an ester substrate and with the Ser^{195}-specific reagent diisopropylfluorophosphate is approximately 10^4 times less than that of the unmodified enzyme. In contrast to the dramatic loss in reactivity of Ser^{195}, the mutant trypsin reacts with the His^{57}-specific reagent, tosyl-L-lysine chloromethylketone, only five times less efficiently than the unmodified enzyme. Thus, the ability of His^{57} to react with this affinity label is not severely compromised. The catalytic activity of the mutant enzyme increases with increasing *p*H so that at *p*H 10.2 the k_{cat} is 6 percent that of trypsin. Kinetic analysis of this novel activity suggests this is due in part to participation of either a titratable base or of hydroxide ion in the catalytic mechanism. By demonstrating the importance of the aspartate residue in catalysis, especially at physiological *p*H, these experiments provide a rationalization for the evolutionary conservation of the catalytic triad.

SERINE PROTEASES FUNCTION IN many biological systems to hydrolyze specific polypeptide bonds. Trypsin, a well-studied member of this family, catalyzes the hydrolysis of peptide and ester substrates that contain lysyl or arginyl side chains. Serine proteases have the triad of residues Asp^{102}, His^{57}, and Ser^{195} at the active site (chymotrypsin numbering system). X-ray crystallographic studies reveal that these three residues are in close proximity, which suggests they may serve as a functional interacting unit responsible for bond formation and cleavage during catalysis (*1*). Numerous chemical and physical studies indicate that Ser^{195} and His^{57} play crucial roles in catalysis. For example, selective reaction of Ser^{195} with diisopropylfluor-

C. S. Craik, Departments of Pharmaceutical Chemistry and of Biochemistry and Biophysics, University of California, San Francisco, San Francisco, CA 94143-0446. S. Roczniak, C. Largman, W. J. Rutter, Hormone Research Institute and Department of Biochemistry and Biophysics, University of California, San Francisco, San Francisco, CA 94143-0448.

*Present address: NutraSweet Company, Mount Prospect, IL 60056.
†Present address: Veterans Administration Hospital, Martinez, CA 94553, and Departments of Internal Medicine and Biological Chemistry, University of California, Davis, CA 95616.